

http://pubs.acs.org/journal/aesccq Article

Multiphase Reactive Bromine Chemistry during Late Spring in the Arctic: Measurements of Gases, Particles, and Snow

Daun Jeong, Stephen M. McNamara, Anna J. Barget, Angela R. W. Raso, Lucia M. Upchurch, Sham Thanekar, Patricia K. Quinn, William R. Simpson, Jose D. Fuentes, Paul B. Shepson, and Kerri A. Pratt*



Cite This: ACS Earth Space Chem. 2022, 6, 2877–2887



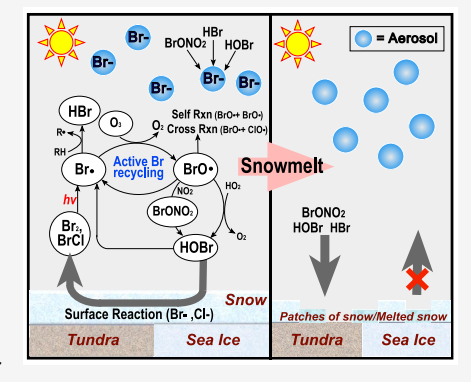
ACCESS

Metrics & More

Article Recommendations

Supporting Information

ABSTRACT: Bromine radicals $(Br\cdot)$ cause ozone depletion and mercury deposition in the Arctic atmospheric boundary layer, following Polar sunrise. These Br radicals are primarily formed by the photolysis of molecular bromine (Br_2) , which is photochemically produced in the snowpack. Recently, it was shown that bromine monoxide $(BrO\cdot)$, formed from the reaction of Br· with ozone, is episodically present until the onset of snowmelt in late Arctic spring. To examine the drivers of this late spring shutdown of reactive bromine chemistry, the gases Br_2 , HOBr, BrO, and BrCl were continuously monitored using chemical ionization mass spectrometry during the spring (March–May 2016) near Utqiagvik, Alaska. On May 10th, all four reactive bromine species fell below levels of detection at the same time that air temperature increased above 0 °C, surface albedo decreased, and snowmelt onset was observed. Prior to the cessation of atmospheric bromine chemistry, local surface snow samples in early May became significantly enriched in bromide, likely due to the slowdown of



reactive bromine recycling with continued deposition but decreased emissions from the snowpack. Particulate bromide concentrations were not sufficient to explain the quantities of reactive bromine gases observed and decreased upon snowmelt. Low wind speeds during the weeks preceding the cessation of reactive bromine chemistry point to the lack of a contribution to bromine chemistry from blowing snow. Together, these results further highlight the significance of the surface snowpack in multiphase bromine recycling with important implications as the melt season arrives earlier due to climate change.

KEYWORDS: atmospheric, troposphere, Polar, aerosol, bromide, sea salt

1. INTRODUCTION

Atmospheric bromine chemistry is prevalent in the springtime polar boundary layer in the Arctic 1-4 and Antarctic. 5 addition to observations of bromine monoxide (BrO·) across regions of sea ice, 8-11 enhanced levels of BrO have also been observed inland up to ~200 km from the coastline. 12 At Alert, Nunavut, Canada following Polar sunrise, Foster et al. measured significantly higher levels of molecular bromine (Br₂) within the snowpack than in the air above, suggesting the snowpack was a source of molecular halogen gases. 13 Since then, several laboratory and field studies have confirmed a photochemical snowpack source of Br₂ and bromine chloride (BrCl). 14-17 These bromine gases are produced from snow that is enriched in bromide (Br-) from the deposition of bromine-containing gases (e.g., hydrobromic acid (HBr), hypobromous acid (HOBr), bromine nitrate (BrONO₂)). ^{18,19} Sea spray aerosol from oceanic wave breaking and open leads contain halide salts that can also deposit onto the surface snowpack. 18-20 Bromine-containing gases can also partition to the particle phase, resulting in aerosol particles with bromide concentrations in excess of sea salt bromide, ²¹ and these bromide-enriched particles can also deposit onto the

surface snowpack. Under sunlit conditions, bromide residing in the liquid-like brine layer (the disordered interface on the snow grain surface) 22 undergoes condensed-phase oxidation, producing Br₂ and BrCl that are subsequently released into the overlying air. 23,24

To explain the high levels of reactive bromine gases observed near the surface, recycling of bromine (R1–R6), involving multiphase reactions on bromide-containing surfaces, is required. Actinic sunlight photolyzes Br_2 and BrCl, releasing highly reactive bromine radicals (Br·) (R1) that can dramatically affect atmospheric composition. Unique to bromine is its ability to oxidize elemental mercury, allowing it to deposit and enter the ecosystem in a more bioavailable form. Bromine radicals also rapidly react with tropo-

Received: June 23, 2022 Revised: November 13, 2022

Accepted: November 14, 2022 Published: November 29, 2022





spheric ozone (O₃), producing BrO (R2) and causing O₃ depletion to near-zero levels. 26,32,33 BrO reacts with HO₂• to produce HOBr (R3), which partitions to the particle or snow grain surface to react with bromide and generate Br₂ or react with chloride to produce BrCl (R6). 34,35 In the presence of nitrogen oxides (NO_x = nitric oxide (NO•) + nitrogen dioxide (NO2•)), BrO can also react to produce BrONO₂ (R4), which undergoes hydrolysis to produce condensed phase HOBr (R5) that subsequently reacts with surface Br⁻ to generate Br₂ (R6). 34,35 BrCl can also be generated in the presence of surface chloride (Cl⁻) 17,24,34,35 or through the cross reaction of halogen oxides (ClO or BrO). 36

$$Br_{2(g)} + h\nu \rightarrow 2Br_{(g)}^{\bullet}$$
 (R1)

$$\operatorname{Br}^{\bullet}_{(g)} + \operatorname{O}_{3(g)} \to \operatorname{BrO}^{\bullet}_{(g)} + \operatorname{O}_{2(g)}$$
 (R2)

$$\operatorname{BrO}^{\bullet}_{(g)} + \operatorname{HO_2}^{\bullet}_{(g)} \to \operatorname{HOBr}_{(g)} + \operatorname{O}_{2(g)}$$
 (R3)

$$\operatorname{BrO}^{\bullet}_{(g)} + \operatorname{NO}_{2(g)} \to \operatorname{BrONO}_{2(g)}$$
 (R4)

$$BrONO_{2(g)} + H_2O_{(1)} \rightarrow HOBr_{(aq)} + HNO_{3(aq)}$$
 (R5)

$$HOBr_{(aq)} + Br_{(aq)}^{-}(or\ Cl_{(aq)}^{-}) + H_{(aq)}^{+}$$

$$\rightarrow Br_{2(g)}(or BrCl_{(g)}) + H_2O_{(l)}$$
(R6)

Atmospheric reactive bromine chemistry is most active during Polar spring. ^{28,37} Measurements at Utqiagvik, AK and Ny Ålesund, Svalbard from 1976 to 1980 consistently showed a summer (June-August) minimum and a spring (February-May) maximum in particulate bromine concentrations.³⁸ Satellite-based spectroscopic measurements suggest that enhanced tropospheric column BrO events are frequent across the Arctic from March to May, retreat northward by June, and are no longer detected by July.³⁹ Burd et al. recently showed the termination of BrO observations upon snowmelt onset in the late spring at Utqiagvik, AK. 40 The lack of BrO after snowmelt underscores the central role that the snowpack plays in the production of halogens throughout the spring. 40 In contrast to the production of Br₂ within the snowpack, oceanic production of sea spray aerosol occurs across the late spring, particularly with sea ice melt in the late spring.⁴¹ Burd et al. explained the phenomenon of termination of BrO upon snowmelt onset by reduced snow surface area, dilution of halides into bulk water upon snowmelt, and hindered snowpack ventilation upon snowmelt. 40 However, the relative importance of these factors, as well as connections to the full bromine multiphase recycling mechanism, remains uncertain.

This study explores the relationship between a suite of atmospheric reactive bromine gases and bromide observed in the surface snowpack and atmospheric particle phase at a coastal Arctic site. Measurements of near-surface atmospheric Br₂, BrO, BrCl, and HOBr were conducted using chemical ionization mass spectrometry near Utqiagvik, Alaska from March to May 2016 as part of the Photochemical Halogen and Ozone Experiment: Mass Exchange in the Lower Troposphere (PHOXMELT). Simultaneously, the surface snowpack and particulate matter were sampled and analyzed for inorganic ion concentrations, providing an opportunity to quantify the contributions of these bromide reservoirs for the production of reactive bromine gases. Our previous work focused on observations and modeling of BrCl to determine the dominant mechanisms of its production that change with solar radiation

through the spring. In this work, we comprehensively examine the gas, particle, and snowpack abundances of bromine with a focus on cessation of reactive bromine chemistry during the late spring snowmelt period.

2. METHODS

2.1. Reactive Bromine Gas Measurements Using Chemical Ionization Mass Spectrometry (CIMS). From March 4 to May 19, 2016, atmospheric HOBr, BrO, Br₂, and BrCl were measured using iodide-CIMS (THS Instruments, Atlanta, GA) at a coastal Arctic tundra site (71.275 °N, 156.641 °W) outside of Utqiagvik, Alaska, as part of the PHOXMELT campaign.^{35,43} Here, we focus on the period prior to and following the onset of snowmelt (April 30-May 19). This CIMS instrument, described in detail by Liao et al., uses iodide-water cluster ions (monitored at m/z 147, IH₂¹⁸O⁻) to react with bromine-containing gases, forming iodide adducts that are then measured by a quadrupole mass analyzer. 44 Chemical ionization occurred in the ion-molecule reaction region, which was humidified to minimize reagent ion and sensitivity fluctuations due to variations in ambient water vapor.44 The CIMS inlet, designed to limit wall losses of reactive gas species, 44-46 was positioned on the building wall at ~1 m above the snowpack and attached via 0.95 cm inner diameter FEP (fluoroethylenepropylene) tubing to a custom three-way valve 44 (held at a constant 30 °C temperature) that enabled online calibrations and background measurements. A total of 37 masses were analyzed every 15 s. Every 15 min, the ambient air flow was diverted through a glass wool scrubber for 4 min to remove the halogen species (>95% efficiency) and attain background measurements. 35,47,48

The reactive bromine species were positively identified by the measured ratio of isotope signals (averaged to 10 min) for each individual species during the campaign. 35,43 For HOBr, signals at m/z 223 (IHO⁷⁹Br⁻) and m/z 225 (IHO⁸¹Br⁻) were observed at a ratio of 1.1 ($R^2 = 0.869$) (theoretical ratio = 1.0). For Br₂, signals at m/z 285 (I⁷⁹Br⁷⁹Br⁻) and m/z 287 $(I^{81}Br^{79}Br^{-})$ were observed at a ratio of 0.53 ($R^2 = 0.933$) (theoretical ratio = 0.51). For BrCl, signals at m/z 241 $(I^{79}Br^{35}Cl^{-})$ and m/z 243 $(I^{79}Br^{37}Cl^{-} + I^{81}Br^{35}Cl^{-})$ were observed at a ratio of 1.2 ($R^2 = 0.70$) (theoretical ratio = 1.3). 43 Unfortunately, m/z 222, corresponding to $I^{79}BrO^{-}$, was not measured. The BrO isotope at m/z 224 (I⁸¹BrO⁻) was measured during the campaign; due to the observed characteristic diurnal behavior of the m/z 224 signal, as well as previous springtime Utqiagvik observations showing minimal isobaric interferences and agreement with multiaxis differential optical absorption spectroscopy (MAX-DOAS) observations, 44,49 we assume this signal can be attributed to ambient BrO.

In the field, Br₂ and Cl₂ were calibrated by sending each gas in N₂ (0.12 L min⁻¹) from its permeation source (VICI Metronics, Inc., Poulsbo, WA) into the CIMS inlet for 2 min every 2 h during ambient sampling. Daily measurements of the Br₂ and Cl₂ permeation rates were performed by bubbling each flow into a 2% potassium iodide solution and measuring the resulting oxidation product, triiodide (I₃⁻), using UV–visible spectrophotometry at 352 nm, ⁴⁴ resulting in campaign average permeation rates of 60 ± 10 ng min⁻¹ Br₂ and 56 ± 8 ng min⁻¹ Cl₂. HOBr at m/z 225 and BrO at m/z 224 were quantified using sensitivity factors relative to Br₂ (at m/z 287) reported by Liao et al. ⁵⁰ BrCl at m/z 243 was quantified using its sensitivity factor relative to Cl₂ (at m/z 199) reported by McNamara et al. ³⁵

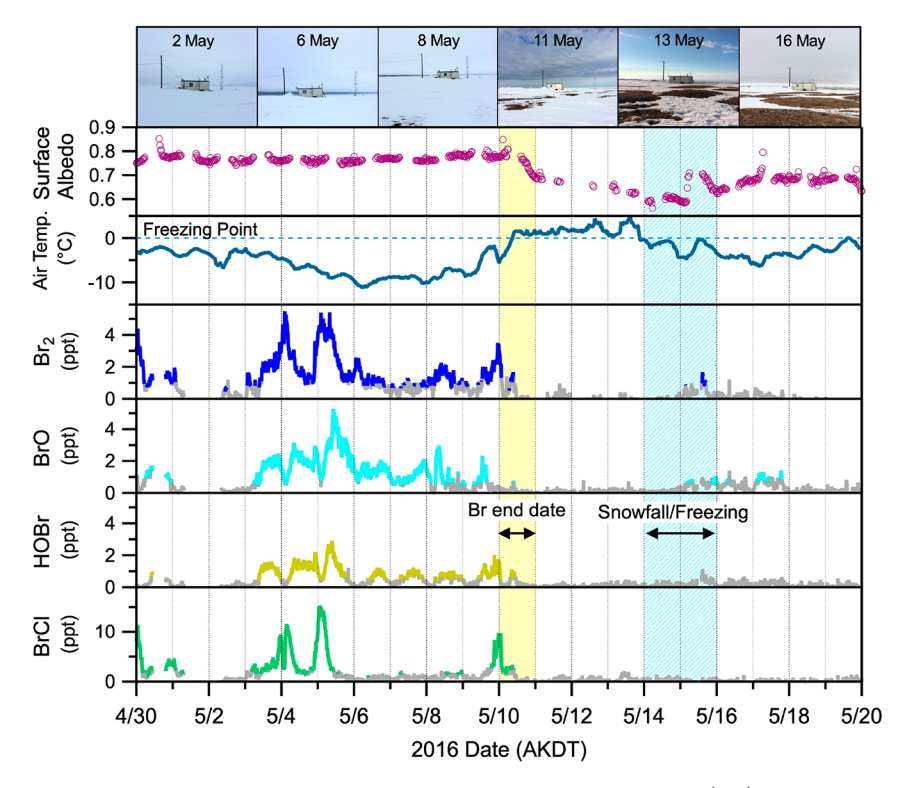


Figure 1. Photographs of the field site show the transformation of the snowpack during snowmelt (top). Surface albedo and air temperature are shown in the upper time series (AKDT; Alaska Daylight Time). The 10 min averaged CIMS measurements of Br_2 , BrO, HOBr, and BrCl mole ratios are shown from April 30 to May 19, 2016, with gray traces representing signals below the CIMS LODs. The horizontal dashed line represents the freezing temperature of H_2O .

The 3σ limits of detection (LODs), corresponding to 4 min background periods, for the quantified masses were 0.8 parts per trillion (ppt, pmol mol⁻¹) for HOBr (m/z 225), 0.8 ppt for BrO (m/z 224), 1 ppt for Br₂ (m/z 287), and 3 ppt for BrCl (m/z 243). Following 10 min averaging, the LODs for HOBr, BrO, Br₂, and BrCl were estimated to be 0.4, 0.4, 0.8, and 2 ppt, respectively, when accounting for counting statistics. The average CIMS measurement uncertainties, including the calibration uncertainties and fluctuations in background signals, for the 10 min averaged HOBr, BrO, Br₂, and BrCl mole ratios were 36% + 0.4 ppt, 40% + 0.4 ppt, 30% + 0.8 ppt, and 41% + 2 ppt, respectively.

2.2. Snowpack and Particulate Inorganic Ion Meas**urements.** The top 1-2 cm of surface snow was sampled at the tundra field site every 3 to 5 days between March 4 and March 29 and every 1 to 3 days from April 2 to May 19 for a total of 41 sampled days. Prior to the onset of snowmelt on May 10, snow depth was measured three times (May 6, 9, and 10), and it ranged from 40 to 55 cm in the sampling locations. After the onset of snowmelt, the remaining patches of soft snow (20-55 cm deep) were sampled until they were mostly melted and only <2 cm of snow were left. The snow samples were collected using a polypropylene scoop, stored doublebagged in polyethylene bags, and kept frozen at $-40~^{\circ}$ C for up to 8 months prior to ion chromatography (IC) analysis. Using IC (Dionex ICS-2100 for anions, Dionex ICS-1100 for cations), the melted snow samples were analyzed in triplicate for meltwater concentrations of the following cations and anions (3 σ LODs in parentheses): Na⁺ (0.07 μ M), K⁺ (0.08 μ M), Mg²⁺ (0.03 μ M), Ca²⁺ (0.13 μ M), NO₃⁻ (0.005 μ M), SO_4^{2-} (0.06 μ M), Cl⁻ (0.03 μ M), and Br⁻ (0.01 μ M). Snow

meltwater pH was measured using a pH meter (Fisher Scientific Accumet AP110).

Submicron ($<1 \mu m$ aerodynamic diameter) and supermicron $(1-10 \mu m)$ atmospheric particles were collected on separate substrates using a multijet cascade impactor with 50% aerodynamic cutoff diameters of 1 and 10 µm and extracted for offline IC analysis following the method of Quinn et al.⁵¹ This sampling was conducted from March 3 to May 18, 2016 at the Barrow Atmospheric Baseline Observatory, part of the National Oceanic and Atmospheric Administration (NOAA) Global Monitoring Laboratory (https://gml.noaa.gov/obop/ brw/), located ~6 km north of the CIMS field site across the flat tundra. A total of 57 submicron samples (collected every ~24 h until May 6, then every ~48 h) and 9 supermicron samples (collected every 6 days until May 5, then every 11 days until May 16) were considered for this study. The LODs for both submicron and supermicron particles following IC analysis were 0.2 ng m⁻³ for Na⁺ and Cl⁻ and 0.1 ng m⁻³ for

Measured snowpack, submicron, and supermicron [Cl⁻], [Br⁻], and [Na⁺] were used to calculate chloride and bromide enrichment factors (EFs; eq E1) following Krnavek et al.⁵²

$$EF_{X} = \frac{[X^{-}]/[Na^{+}]_{\text{snow or particle}}}{[X^{-}]/[Na^{+}]_{\text{seawater}}}$$
(E1)

X refers to Cl^- or Br^- , and 1.17 and 0.0018 are the seawater molar ratios of $[Cl^-]/[Na^+]$ and $[Br^-]/[Na^+]$, respectively.⁵³

2.3. Auxiliary Measurements. Ozone was measured using a gas analyzer (model 205, 2B Technologies Inc., Boulder, CO) that subsampled the air stream from the CIMS inlet (Section 2.1) at 1.3 L min⁻¹. Wind speed, wind direction,

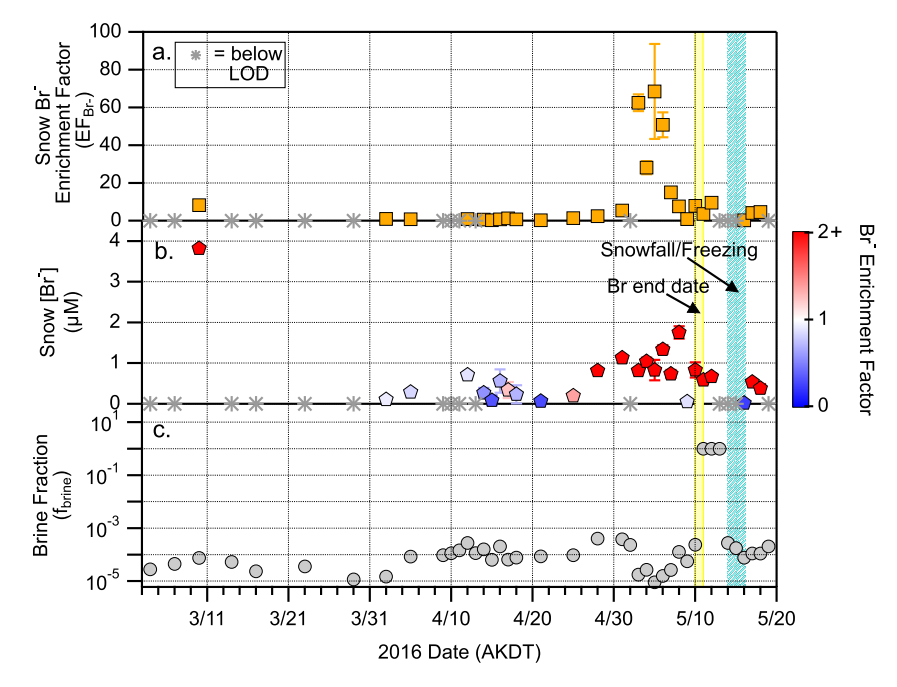


Figure 2. Bromide enrichment factor (a) and bromide (b) in surface snow from March 4 to May 19, 2016. Gray asterisks represent data below the detection limit, and error bars represent standard deviations for triplicate measurements. The color scale (b) represents bromide enrichment factors (EF, eq E1), also shown in panel a, with the color scale here only up to 2 for visual purposes. Snow brine fraction (f_{brine} ; c), shown with a log scale, was calculated for each snow sample using the Cho et al. ⁶¹ parametrization using measured [Na⁺], [Cl⁻], and air temperature.

and solar radiation were measured at the CIMS field site. 35,43 Wind speed and wind direction were measured with a propeller anemometer (model 05103, RM Young, Traverse City, MI) placed on a tower at ~11.5 m above the surface, and solar radiation was measured with a pyranometer (part of model CNR1, Kipp & Zonen, Delft Holland) mounted on a tower at ~3 m above the surface. Air temperature, at ~2 m above ground level, was measured at the NOAA Observatory, and surface albedo data (spectral surface albedo product produced from multifilter radiometer measurements) were provided by the Atmospheric Radiation Measurement (ARM) Climate Research Facility, located adjacent to the NOAA Observatory.

3. RESULTS AND DISCUSSION

3.1. Shutdown of Reactive Bromine Chemistry in Late **Spring upon Snowmelt.** Figure 1 shows gas-phase BrCl, HOBr, Br₂, and BrO CIMS measurements from April 30 to May 19, 2016. Snow surface albedo and air temperature are also shown as proxies for the snowmelt onset period. Photographs taken at the sampling site visually show the onset of snow melting on May 10 as the air temperature rose above freezing (>0 °C) and the snowmelt exposed the underlying Arctic tundra. The sudden decrease in snow surface albedo from 0.8 to <0.7 on May 10 due to snowmelt was accompanied by an immediate decrease in the mole ratios of all four measured reactive bromine gases (Br2, BrO, HOBr, and BrCl). From March 4 to May 10, daily maxima in Br₂, BrO, HOBr, and BrCl ranged from 1 to 11, 0.2 to 8, 0.4 to 4, and 1 to 21 ppt, respectively (Figure S3). After May 10, HOBr and BrCl signals stayed below their LODs (0.4 and 2 ppt, respectively). Br₂ and BrO were mostly below LODs (3 and 1 ppt, respectively) with only brief periods, discussed below, that were slightly above their LODs but below their limits of quantitation.

Our observations support the results described by Burd et al. who conducted concurrent BrO measurements at Utqiagvik, AK using MAX-DOAS. 40 Using BrO, they defined the "end date" of the reactive bromine season at Utqiagvik as May 7 with the "melt onset date" as May 10, defined as the first date for which air temperatures reached 0 °C.40 The difference between the May 7 and 10 end dates for 2016 in Burd et al. 40 and our study is likely due to differences in the LODs of the two instrumental techniques (MAX-DOAS and CIMS). For the end date, Burd et al. used a threshold of 5×10^{13} molecules cm⁻² for the differential slant column density (dSCD) of BrO at 1° of elevation. 40 For our study, we used the CIMS BrO LOD (0.8 ppt) as the threshold, which extended the BrO observations from May 7 to 10 (Figure 1). Our observations of additional reactive halogen species BrCl, HOBr, and Br2 further corroborate the cessation of bromine chemistry at the onset of spring snowmelt on May 10.

After the May 10th end date, BrO and Br2 were observed slightly above the CIMS LODs (0.4 and 0.8 ppt, respectively) between May 15 and 17. During this time, air temperatures fell below freezing (reaching $-6~^{\circ}\text{C}$) and did not increase above 0 °C until May 19 (Figure 1). Burd et al.40 also found that air temperatures below 0 °C, in conjunction with light snowfall, were associated with a resumption of reactive bromine production, which they observed from BrO levels during several periods in late spring 2012, 2014, and 2015 at Utqiagvik. The recurrences we observed during our study also followed periods of light snowfall on May 14 and 15, 2016. The previously reported MAX-DOAS BrO observations approached or very slightly exceeded their measurement threshold during this time period in 2016.⁴⁰ The consistency between Burd et al. 40 and our results further confirms that the onset of snowmelt is what drives the end of active bromine chemistry.

The elevated halogen mole ratios in early May, as well as their sudden decrease on May 10, were not associated with wind speed fluctuations (Figure S1). From April 30 to May 19, wind speeds were consistently low to moderate, averaging $5 \pm 2 \text{ m s}^{-1} (\pm 1\sigma)$ and below the typical 8 m s⁻¹ threshold for blowing snow to occur. An addition, there was no correlation ($R^2 = 0.006$) between vertical eddy diffusivity ($K_{\rm m}$), which depends on atmospheric stability and friction velocity (u_*), and Br₂ mole ratios (Figures S1 and S2). Further, the eddy diffusivity between Apr 30 and May 15 remained low and varied little with an average of $0.07 \pm 0.04 \text{ m}^2\text{s}^{-1}$ (excluding the two short (<3 h) peaks on May 6 and 9), suggesting that the dispersion of gases in the atmospheric boundary layer also did not explain the decreased levels of reactive bromine upon snowmelt.

While our focus is on atmospheric bromine chemistry, we note that reactive chlorine chemistry continued after May 10, suggesting decoupled bromine and chlorine production mechanisms during this time. McNamara et al. reported observations of molecular chlorine (Cl₂) and nitryl chloride (ClNO₂) until May 14, 2016.⁴³ The period of May 8–14, 2016 was influenced by local town (Utqiagʻvik) pollution and air mass transport from the North Slope of Alaska oilfields. The polluted air mass also contained enhanced levels of dinitrogen pentoxide (N₂O₅), a precursor for ClNO₂.⁴³ McNamara et al. hypothesized that the photolysis of ClNO₂ could provide an alternate source of Cl radicals for multiphase Cl₂ recycling.⁴³

3.2. Enhanced Snowpack Bromide in May Suggests **Deposition of Bromine-Containing Gases.** The sampled snow (1-2 cm) encompasses the top layer of the snowpack (~1 mm) where modeling suggests that atmospheric recycling of bromine occurs.⁵⁵ In addition, photochemical snowpack production of molecular halogens occurs below the surface of the snowpack; Custard et al.²⁴ previously measured ppb (nmol mol⁻¹) levels of Br₂ in the interstitial air at a snowpack depth of 10 cm, in agreement with the previously measured e-folding depth of 14 cm. 56 Near the end of the active Br recycling (May 1-12), surface snow samples collected at the PHOXMELT field site were significantly enriched in bromide compared to seawater (Figure 2). A calculated bromide enrichment factor $(EF_{Br}^-$, eq $E1)^{57}$ of greater than 1 means more bromide is present than can be explained by seawater/fresh sea spray aerosol influence alone, while an EF_{Br}- lower than 1 is indicative of lower concentrations of bromide compared to that expected from seawater influence (i.e., depleted in bromide). The EF_{Br}- shows the cumulative history of the snowpack as both a source and sink of bromine-containing gases. Cumulative sourcing of reactive halogen gases from the snowpack leads to net halide depletion in snowpack, while deposition to the snowpack pushes the balance toward halide enrichment.¹⁹ Snowpack bromide and chloride enrichment is indicative of the net deposition of halogen-containing gases, such as HBr, HCl, HOBr, HOCl, BrONO₂, and ClONO₂. 57-59 Fresh snow collected in Alert, Canada, was previously observed to quickly become enriched in bromide due to deposition of bromine-containing gases during springtime. 60 The deposition of bromide-enriched aerosol particles, discussed in Section 3.3, also increases snowpack EF_{Br}-.²¹ Simpson et al.⁵⁹ showed increasing bromide enrichment in the Arctic tundra surface snowpack with distance inland, consistent with the deposition of these bromine-containing gases. Peterson et al. 19 previously also found surface snow in first-year ice regions to typically be

enriched in bromide, whereas surface snow above multiyear sea ice was typically depleted in bromide, relative to seawater.

Before April 30 (March 4-April 28), snowpack bromide was often depleted compared to seawater (EF_{Br}-: range of 0.01-8, average of 1 ± 2 with data below the LOD set as $LOD \times 0.5$)⁶² (Figure 2); yet, Br₂ was observed, ranging from daily maxima of 2–11 ppt (Figure S3). During this period, surface snow Br⁻ concentrations ranged from below the LOD (0.01 μ M) to 4 μM (average 0.3 \pm 0.8 μM). This illustrates that bromine recycling reactions were active, and the snowpack served as both a sink and a source leading to changes in EF_{Br}-. In comparison, during early May (May 1-8), the surface snowpack EF_{Br}- ranged from 0.02 to 68 (average of 30 \pm 27) with snowmelt [Br⁻] ranging from below the LOD (0.01 μ M) to 2 μ M (average of 1.0 \pm 0.5). Notably, the highest snowpack bromide concentrations of the spring (March-May) were observed with the highest EF_{Br}- values. As discussed below, this highlights that the deposition of brominecontaining gases to the snowpack during this early May period controlled the snowpack bromide concentrations. To a lesser extent, snowpack chloride was also enriched (EF_{Cl}⁻ ~ 1 to 2) during this period (Figure S4) as previously observed in the Arctic springtime. 19,57 This maximum snowpack halide enrichment coincides with the period just before the ultimate shutdown of reactive bromine gas production, when Br2, BrCl, and BrO were relatively high (May 4 and 5, as shown in Figure

As shown in Figure 2, the elevated surface snow Br-enrichment factors and presence of Br₂ are consistent with snowpack production. Previous observations have shown Br₂ production from sunlit surface snowpacks above both tundra and sea ice. These surface snowpacks had lower salinity, lower pH, and higher Br⁻ to Cl⁻ ratios than sea ice, brine icicles, and basal snow collected directly above sea ice that was influenced by brine migration and did not produce detectable Br₂. Overall, the snowpack production of reactive bromine gases depends on various factors (e.g., [Br⁻] at the snow grain surface, pH, rates of competing halogen reactions). The enrichment of snow in bromide is expected to assist in the production of Br₂ upon snowpack illumination and/or the reaction of BrONO₂ or HOBr. Ts,17,24,63–65

After the onset of snowmelt, total ion concentrations of surface snow samples, collected from the remaining patches of snow from May 11 to 20, decreased to their lowest levels (<180 μ M, Figure S5). The EF $_{\rm Br}$ - of the remaining snow after May 10 was briefly >1 (enriched) (Figure 2). Upon the arrival of fresh snowfall and below-freezing temperatures, the snow became depleted in bromide (EF $_{\rm Br}$ - < 1) due to snowpack reactive bromine gas production, as evidenced by detectable Br $_2$ and BrO (Figure 1). Finally, the snow became enriched (EF $_{\rm Br}$ - > 1) again (Figure 2), likely from the deposition of bromine-containing species with limited reactive bromine gas production (Figure 1). Overall, May 11 to 20 had EF $_{\rm Br}$ - values ranging from 0.04 to 10 with an average of 2 \pm 3, which was lower than that in the early May period.

The snow grain brine fraction $(f_{\rm brine})$ was estimated using the Cho et al. ⁶¹ parametrization for each snow sample. This is calculated based on the measured snow [Na⁺] and [Cl⁻] and the average air temperature for each snow sampling day (Figures 2 and S6). A larger brine fraction implies more liquid water is present at the surface of the snow grain with a $f_{\rm brine}=1$ representing complete melting. Here, $f_{\rm brine}$ was set to 1 if the ambient temperature reached or exceeded 273 K. However,

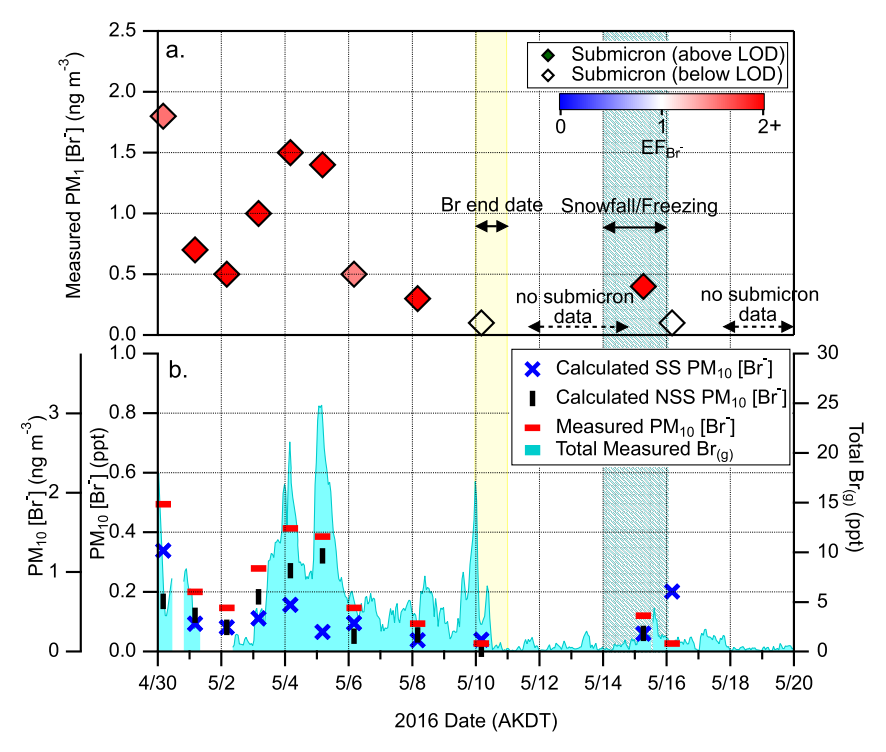


Figure 3. Time series (April 30–May 19, 2016) of (a) submicron (PM₁) particulate bromide (Br⁻) concentrations and (b) comparison of total (PM₁₀) sea salt (SS), non-sea salt (NSS), and measured particulate bromide with total measured bromine gases ($T_{Br(g)}$). Supermicron (PM₁₋₁₀) bromide concentrations were below LOD during this period. PM₁ and PM₁₋₁₀ bromide concentrations during the whole study are shown in Figure S7. The duration of PM₁ sample collection was 1 day prior to May 6 and 2 days afterward. The duration of the PM₁₋₁₀ sample collection was 6 days prior to May 5 and 11 days afterward. Dashed lines with arrowheads represent periods when submicron samples were unavailable. Bromide enrichment factors (EF_{Br}⁻) for submicron particles are color coded. Due to the differences in the sampling times between PM₁ and PM₁₋₁₀, total (PM₁₀) calculated SS (blue), calculated NSS (black), and measured bromide (red) were estimated by adding the PM₁₋₁₀ [Br⁻] to the daily PM₁ [Br⁻] within each PM₁₋₁₀ sampling period. Total measured Br gas (light blue) was estimated by adding all measured bromine gas species (1 h averaged, below LOD included) during the study (i.e., $T_{Br(g)} = 2 \times Br_2 + BrO + HOBr + BrCl$).

this is an overestimation because the entire snowpack does not immediately melt at this temperature, since the snowpack temperature is likely lower than the air above (e.g., from radiational cooling and the latent heat of fusion for the phase transition from solid to liquid). Prior to the three abovefreezing days (May 11–13), f_{brine} averaged 0.0001 from March 4 to May 10 (Figures 2 and S6). Between May 11 and 13, the temperature rose above freezing (3.1 \pm 0.4 °C) with the brine fraction set as 1 to reflect the occurrence of snowmelt (Figures 2 and S6). However, as shown in the photos of the field site in Figure 1, the ambient temperature above freezing did not result in full snowpack melt, and therefore, the remaining patches of snow were sampled for analysis. A larger brine fraction indicates a higher water content, which in turn lowers the available surface area of the snowpack due to coalescence of snow grains⁶⁶ and changes in snow grain morphology, hindering reactivity.⁶⁷ Moreover, increased liquid water content, given a fixed amount of ions in the snow, decreases the concentration of halides⁶⁸ through dilution of the surface halides in the liquid environment and may increase the pH⁶⁹ at the snow grain surface, resulting in decreased heterogeneous reactivity.

Between May 14 and 19, the average air temperature (-2.9 ± 1.6 °C) fell below the freezing point, and $f_{\rm brine}$ was calculated to be 2 (± 0.7) × 10^{-4} (Figures 2 and S6). However, the observed reactive bromine gases did not recover to the levels observed prior to the snowmelt (Figure 1). This result is similar to the observation by Burd et al., 40 who found that the below-freezing temperature itself was not sufficient to induce

the recurrence of bromine recycling and additional conditions, for example, new snowfall, were required. This could be due to limited ventilation within the refrozen snowpack and the redistribution of ions upon snowmelt that hinders its availability at the surface for heterogeneous reactions. Indeed, after the first onset of snowmelt, the total snowpack inorganic ion concentration dropped (Figure S5), consistent with the expected loss of ions as a result of brine drainage from the snowpack. Moreover, the refreezing of the snowpack may result in bromide ions migrating to atmospherically inaccessible brine pockets or grain boundaries that hinder their heterogeneous reactivity with atmospheric gases. ⁶⁷

3.3. Particulate Bromide Is Insufficient for Reactive Bromine Production. Bromide-containing particles can also be a source of bromine-containing gases, causing particulate bromide concentrations to decrease. During the March–May 2016 sampling period, most (range 73–99%, average 83 \pm 6%) of the measured PM₁₀ (particulate matter with diameters <10 μ m) bromide was in the submicron range (<1 μ m in diameter). Throughout the March–May 2016 sampling period, the concentrations of bromide ranged from below the LOD (0.1 ng m⁻³) to 0.3 ng m⁻³ for PM₁₋₁₀ and below the LOD (0.1 ng m⁻³) to 25 ng m⁻³ for PM₁ (Figure S7). The majority (\sim 72%) of submicron particle samples were enriched in bromide (EF_{Br}- ranging from 0.3 to 48, average 3 \pm 7), while none of the supermicron (1–10 μ m) samples were enriched in bromide relative to seawater (Figure 3). Similar to the snowpack, excess bromide, relative to seawater, is from the partitioning of reactive bromine-containing gases to the

particle phase. 21,38 Previous measurements during the Arctic spring have shown the enrichment of bromide in submicron particles and depletion of bromide in coarse mode particles. ^{2,21,38,75} This indicates that bromide enrichment is through gas to particle partitioning of bromine-containing gases (e.g., HBr, HOBr, BrONO₂).²¹ A study by Hara et al.⁷ at Ny-Ålesund, Svalbard in the winter-spring found that most of the excess bromide was found in particles <2.3 μ m in diameter. Another study by Sturges and Barrie collected particles (<20 µm) in three locations in the Canadian Arctic for five years (1979-1984). The study reported excess bromine in the springtime that could not be explained by known particle sources and ascribed it to partitioning of gaseous bromine produced from nonparticulate sources.⁷⁵ In the current study, the measured gas-phase bromine could not be explained by particulate bromide alone (as explained below), and therefore, the enrichment of bromide in submicron aerosol particles prior to snowmelt is consistent with snowpack-produced Br₂ and BrCl, leading to atmospheric bromine recycling and the gas-particle partitioning of brominecontaining gases (e.g., HBr, HOBr, BrONO₂).

The slowdown of reactive bromine chemistry beginning in late April through the end of the study is evident in the measured particulate [Br⁻] (Figure 3a). Prior to the onset of snowmelt (April 30-May 10), submicron particle bromide was elevated (0.3-2 ng m⁻³), compared to the levels after the snowmelt. Following snowmelt, two of the three submicron samples from May 10 to 18, as well as the supermicron sample from May 5 to 16, did not have detectable levels of bromide (Figures 3a and S7), despite the increased sampling durations during this period. This further supports limited atmospheric bromine recycling following snowmelt. Notably, the only submicron sample with detectable bromide was collected at the time of the below-freezing temperatures and light snowfall on May 14-15. Previous studies have shown that the partitioning between particulate bromide and gas-phase bromine can be influenced by O_3 concentration. S5,78 After the onset of snowmelt, measured O₃ ranged from 10 to 35 ppb with no sustained periods of ozone depletion (Figure S3), while both particulate bromide and gas-phase reactive bromine remained low. Therefore, the reduced bromine levels are likely not explained by the ambient O₃ levels.

In the Arctic, particulate bromide originates from the seawater and can be incorporated into atmospheric particles through two main processes: (1) direct generation of sea spray (e.g., wave breaking and bubble bursting in open leads) 18,59 and (2) gas-particle partitioning of bromine-containing gases (e.g., HBr, HOBr, BrONO $_2$). 21,75 It has also been hypothesized that sublimation of suspended blowing snow particles could be a particulate bromide source at high wind speed conditions. $^{79-82}$ To estimate the particulate bromide available for production of reactive bromine-containing gases, sea salt and non-sea salt bromide concentrations (Figure 3b) were calculated via eqs E2 and E3 using measurements of Br $^-$ and Na $^+$ in PM $_1$ and PM $_{1-10}$. 21

$$[Br^{-}]_{sea \ salt} = 0.0018 \times [Na^{+}]$$
 (E2)

$$[Br]_{\text{non-sea salt}} = [Br]_{\text{total}} - 0.0018 \times [Na^{+}]$$
 (E3)

In this equation, 0.0018 represents the Br $^-$ /Na $^+$ molar ratio in seawater. ⁸³ An excess of particulate bromide ([Br $^-$]_{non-sea salt} > 0), compared to seawater, is from the partitioning of gas-phase bromine to the particle phase. ^{21,38} Note that in eq E3

 $[Br^-]_{non\text{-}sea\ salt}$ becomes negative when bromide is depleted with respect to the ratio in seawater due to the production of bromine-containing gases. In these cases, $[Br^-]_{non\text{-}sea\ salt}$ was assumed to be zero for the calculation of total PM_{10} non-sea salt Br^- .

Assuming that all non-sea salt and sea salt Br is available to produce gas-phase bromine, particulate Br was not sufficient to explain the observed reactive bromine species $(T_{Br(g)})$ (Figure 3b). From April 30 to May 10, the average mass concentration of total non-sea salt Br $^-$ from particles < 10 μ m $(PM_{10} = PM_1 + PM_{1-10})$ was calculated to be 0.5 ± 0.4 ng m⁻³ (range 0.03-1.2 ng m⁻³). The maximum of 1.2 ng m⁻³ on May 5 corresponded to a local maximum in reactive gas-phase bromine (Figure 3b). During this period (April 30 to May 10), the average mass concentration of total sea salt PM $_{10}$ was 0.4 \pm 0.3 ng m^{-3} (range $0.1-1.3 \text{ ng m}^{-3}$) with the maximum on April 30. When converted to ppt, the maximum non-sea salt (1.2 ng m^{-3}) and sea salt (1.3 ng m^{-3}) bromide concentrations each correspond to a maximum of only 0.3 ppt. This is far below the mole ratios of the total observed reactive bromine species ($T_{Br(g)} = 2 \times Br_2 + BrO + HOBr + BrCl$) between April 30 and May 10 (ranged from below LOD to 25 ppt; average 7 ± 5 ppt, considering 1 h data) (Figure 3b). Note that $T_{Br(g)}$ only corresponds to the measured compounds and does not include gas-phase HBr, for example, which has been previously measured to be 4-17 ppt in the springtime Arctic. 84,85 Li et al. 86 previously estimated HBr to typically be ∼1% of total gaseous inorganic bromine during springtime at Alert, Canada. When considering the maximum total measured (PM₁₀) bromide, which includes both sea salt and non-sea salt bromide, of 0.9 ± 0.6 ng m⁻³ (range 0.1-1.8 ng m⁻³), the maximum available bromine of 0.5 ppt is still not sufficient to explain the reactive bromine gas levels (Figure 3b). This result is similar to the previous particulate and gasphase inorganic bromine observations reported by Berg et al.³⁸ and Barrie et al.,⁸⁷ in which springtime particulate bromide was typically 4 to 18 times lower than the measured total gaseous inorganic bromine in Utqiagvik, Alaska and Alert, Canada, respectively.

The limited available particulate Br^- shows that another source is needed to explain the reactive bromine gas observations. Following the approach of Guimbaud et al., we calculate the maximum gas phase mole ratio of Br_2 that could theoretically be produced and released into the atmospheric surface layer above the snowpack during the May 1-10 period. We calculate, via eq E4, the potential gas phase Br_2 concentration in the air overlying the snowpack and into which the snowpack-produced Br_2 mixes.

$$[Br_2]_{(max),ppb} = \frac{1 \text{ mol } Br_2}{2 \text{ mol } Br} \times \chi_{Br}^- \times 10^9 \times (Z^* \times N_a')^{-1}$$
(E4)

Here $\chi_{\rm Br}^-$ is the number of moles per unit surface area (m⁻²), which is the atmospheric column molecular density of measured snowpack bromide. Z^* (2.2 m) is the effective mixing height for Br₂ released from the surface, ⁸⁸ calculated as $(K_{\rm m} \cdot \tau)^{0.5}$, where $K_{\rm m}$ is the vertical scale eddy diffusivity (average of 0.07 m²s⁻¹, Figure S1) and τ is the atmospheric lifetime of Br₂, taken as $J_{\rm Br2}^{-1}$ or 71 s (the daytime average). N_a' is the number (22.0) of moles of air m⁻³ at 268 K (average temperature), and 10⁹ converts to units of gas phase mole ratio, ppb (nmol mol⁻¹). Previous observations in Utqiaġvik measured an e-folding depth for radiation penetration into the

tundra snowpack to be ~14 cm. 56 The measured average surface (top $\sim 1-2$ cm) snow [Br⁻] was 9.5×10^{-7} M. The snow [Br-] is highest at the surface from deposition of bromine-containing gases and particles, 18 and our previous snow depth profile measurements at this tundra site show that we expect that the average concentration through the top 14 cm of the photic zone of the snowpack is expected to be approximately half the surface concentration.⁸⁹ We further assume that the snow volume fraction = 0.4 and that 10% of the snowpack Br is accessible to exchange with the atmosphere (e.g., not buried within ice grains during metamorphosis⁶⁷). Through this calculation, we obtain χ_{Br} = 2.7×10^{-6} moles m⁻². Then, from eq E4, we obtain the potential to produce 28 ppb of Br₂ mixed throughout that 2.2 m deep overlying atmosphere, which is 5600 times the observed Br₂ (average 5 ppt). While this is an order of magnitude estimate of the available Br2 that could be photochemically produced in the snowpack and released into the overlying surface layer of the atmosphere, the result obtained makes it clear that there is an abundant supply of snow Br⁻ that can account for the observations from a surface Br₂ flux. We note that the snowpack is continually replenished with Br from the dry deposition of particles and gas-phase bromine (e.g., HBr and HOBr). The release of gases from the snowpack interstitial air to the overlying atmosphere depends on wind pumping, which flushes the interstitial air out of the snowpack. 90,91 Low to moderate wind speeds $(4 \pm 2 \text{ m s}^{-1})$ prevailed during this period, as shown in Figure S1. We used a conservative value of the fraction of snow-phase Br available for oxidation and exchange with the atmosphere (0.1), similar to previous work involving snow [I⁻] and I₂ production.⁹² Custard et al.²⁴ previously measured hundreds of ppbs of Br₂ in the snowpack interstitial air at a depth of 10 cm, showing the significant photochemical production of Br₂ within the snowpack, and the large concentration gradient that then drives the flux of Br2 into the overlying atmosphere. Wang and Pratt³⁴ derived similar Br₂ emission fluxes from the snowpack as those measured by Custard et al. 24 (on the order of $1-12 \times$ 108 molecules cm⁻² s⁻¹), and these were able to explain the observed ambient Br₂ above the snowpack.

4. CONCLUSIONS

The late-spring observations of reactive bromine gases coincident with the measurement of surface snowpack and particulate bromide provide a unique case study for examining the sources and seasonality of Arctic reactive bromine chemistry. Following the onset of snowmelt due to rising temperatures on May 10, all four reactive bromine gases measured (Br₂, BrO, HOBr, and BrCl) fell to below detection limits. The shutdown of the production and recycling of these species shows the snowpack as the dominant source for bromine gases. The bromide concentration within the particle phase was insufficient to explain the reactive bromine gas observations, while the surface snowpack could theoretically produce well over the amount of observed Br₂ in the air above the snowpack. Given the rapid decline in sea ice coverage and warming of the Arctic region, it is likely that the shutdown of reactive bromine chemistry will occur earlier in spring with earlier snowmelt onset. 93-95

ASSOCIATED CONTENT

Supporting Information

The Supporting Information is available free of charge at https://pubs.acs.org/doi/10.1021/acsearthspace-chem.2c00189.

Time series plots of meteorological parameters, O_3 , bromine-containing gases, surface snow pH, inorganic ion concentrations, and calculated snow brine fractions, EF_{Cl} , and EF_{Br} ; plot of $[Br_2]$ versus eddy diffusivity (PDF)

AUTHOR INFORMATION

Corresponding Author

Kerri A. Pratt — Department of Chemistry, University of Michigan, Ann Arbor, Michigan 48109, United States; Department of Earth and Environmental Sciences, University of Michigan, Ann Arbor, Michigan 48109, United States; orcid.org/0000-0003-4707-2290; Phone: (734) 763-2871; Email: prattka@umich.edu

Authors

Daun Jeong — Department of Chemistry, University of Michigan, Ann Arbor, Michigan 48109, United States; orcid.org/0000-0001-7703-5226

Stephen M. McNamara — Department of Chemistry, University of Michigan, Ann Arbor, Michigan 48109, United States

Anna J. Barget – Department of Chemistry, University of Michigan, Ann Arbor, Michigan 48109, United States

Angela R. W. Raso — Department of Chemistry, University of Michigan, Ann Arbor, Michigan 48109, United States; Department of Chemistry, Purdue University, West Lafayette, Indiana 47907, United States

Lucia M. Upchurch — Cooperative Institute for Climate, Ocean, and Ecosystem Studies, University of Washington, Seattle, Washington 98105, United States; Pacific Marine Environmental Laboratory, National Oceanic and Atmospheric Administration, Seattle, Washington 98115, United States; orcid.org/0000-0003-1351-6332

Sham Thanekar – Department of Meteorology and Atmospheric Science, Pennsylvania State University, University Park, Pennsylvania 16802, United States

Patricia K. Quinn — Pacific Marine Environmental Laboratory, National Oceanic and Atmospheric Administration, Seattle, Washington 98115, United States

William R. Simpson – Department of Chemistry and Biochemistry and Geophysical Institute, University of Alaska Fairbanks, Fairbanks, Alaska 99775, United States

Jose D. Fuentes – Department of Meteorology and Atmospheric Science, Pennsylvania State University, University Park, Pennsylvania 16802, United States

Paul B. Shepson — Department of Chemistry and Department of Earth, Atmospheric, and Planetary Sciences & Purdue Climate Change Research Center, Purdue University, West Lafayette, Indiana 47907, United States; School of Marine & Atmospheric Sciences, Stony Brook University, Stony Brook, New York 11790, United States

Complete contact information is available at: https://pubs.acs.org/10.1021/acsearthspacechem.2c00189

Author Contributions

 $^{
m O}$ D.J. and S.M.M. contributed equally to this work.

Notes

The authors declare no competing financial interest.

ACKNOWLEDGMENTS

Financial support was provided by the National Science Foundation (PLR-1417668, PLR-1417906, PLR-1417914, OPP-2000493, OPP-2000428, OPP-2000403, OPP-2001449). L.M.U. acknowledges the Cooperative Institute for Climate, Ocean, and Ecosystem Studies (CIOCES) under NOAA Cooperative Agreement NA20OAR4320271 (Contribution No. 2022-1211). S.M.M. and A.J.B. were partially funded by Michigan Space Grant Consortium Graduate and Undergraduate Research Fellowships, respectively. We thank UIC Science and Polar Field Services as well as Dandan Wei and Jesus Ruiz-Plancarte (Penn State University) for field logistical support in Utqiagvik. The NOAA Earth System Research Laboratory Global Monitoring Division (http://esrl. noaa.gov/gmd/) is acknowledged for supplementary radiation and air temperature data from the Barrow Observatory. Surface albedo data were provided by the ARM Climate Research Facility, a US Department of Energy Office of Science user facility sponsored by the Office of Biological and Environmental Research. We thank Qianjie Chen (University of Michigan) for the calculation of eddy diffusivities and discussions as well as Siyuan Wang (NCAR) and Natasha M. Garner (University of Michigan and University of Calgary) for discussions. This is PMEL contribution number 5385.

REFERENCES

- (1) Barrie, L. A.; Bottenheim, J. W.; Schnell, R. C.; Crutzen, P. J.; Rasmussen, R. A. Ozone Destruction and Photochemical Reactions at Polar Sunrise in the Lower Arctic Atmosphere. *Nature* **1988**, 334 (6178), 138–141.
- (2) Oltmans, S. J.; Schnell, R. C.; Sheridan, P. J.; Peterson, R. E.; Li, S. M.; Winchester, J. W.; Tans, P. P.; Sturges, W. T.; Kahl, J. D.; Barrie, L. A. Seasonal Surface Ozone and Filterable Bromine Relationship in the High Arctic. *Atmospheric Environment* (1967) 1989, 23 (11), 2431–2441.
- (3) Simpson, W. R.; Brown, S. S.; Saiz-Lopez, A.; Thornton, J. A.; Von Glasow, R. Tropospheric Halogen Chemistry: Sources, Cycling, and Impacts. *Chem. Rev.* **2015**, *115* (10), 4035–4062.
- (4) McConnell, J. C.; Henderson, G. S.; Barrie, L. A.; Bottenheim, J. W.; Niki, H.; Langford, C. H.; Templeton, E. M. J. Photochemical Bromine Production Implicated in Arctic Boundary-Layer Ozone Depletion. *Nature* **1992**, 355, 150–152.
- (5) Buys, Z.; Brough, N.; Huey, L. G.; Tanner, D. J.; Von Glasow, R.; Jones, A. E. High Temporal Resolution Br2, BrCl and BrO Observations in Coastal Antarctica. *Atmos Chem. Phys.* **2013**, *13*, 1329–1343.
- (6) Frieß, U.; Hollwedel, J.; König-Langlo, G.; Wagner, T.; Platt, U. Dynamics and Chemistry of Troposheric Bromine Explosion Events in the Antarctic Coastal Region. *Journal of Geophysical Research D: Atmospheres* **2004**, *109* (D6), 1–15.
- (7) Kreher, K.; Johnston, P. V.; Wood, S. W.; et al. Ground-Based Measurements of Tropospheric and Stratospheric BrO at Arrival Heights, Antarctica. *Geophys. Res. Lett.* **1997**, *24* (23), 3021–3024.
- (8) Wagner, T.; Platt, U. Satellite Mapping of Enhanced BrO Concentrations in the Troposphere. *Nature* **1998**, 395 (6701), 486–490.
- (9) Richter, A.; Wittrock, F.; Eisinger, M.; Burrows, J. P. GOME Observations of Tropospheric BrO in Northern Hemispheric Spring and Summer 1997. *Geophys. Res. Lett.* **1998**, 25 (14), 2683–2686.
- (10) Koo, J. H.; Wang, Y.; Kurosu, T. P.; Chance, K.; Rozanov, A.; Richter, A.; Oltmans, S. J.; Thompson, A. M.; Hair, J. W.; Fenn, M. A.; Weinheimer, A. J.; Ryerson, T. B.; Solberg, S.; Huey, L. G.; Liao, J.; Dibb, J. E.; Neuman, J. A.; Nowak, J. B.; Pierce, R. B.; Natarajan,

- M.; Al-Saadi, J. Characteristics of Tropospheric Ozone Depletion Events in the Arctic Spring: Analysis of the ARCTAS, ARCPAC, and ARCIONS Measurements and Satellite BrO Observations. *Atmos Chem. Phys.* **2012**, *12* (20), 9909–9922.
- (11) Simpson, W. R.; Carlson, D.; Hönninger, G.; Douglas, T. A.; Sturm, M.; Perovich, D.; Platt, U. First-Year Sea-Ice Contact Predicts Bromine Monoxide (BrO) Levels at Barrow, Alaska Better than Potential Frost Flower Contact. *Atmos Chem. Phys.* **2007**, *7* (3), 621–627.
- (12) Peterson, P. K.; Pöhler, D.; Zielcke, J.; General, S.; Frieß, U.; Platt, U.; Simpson, W. R.; Nghiem, S. V.; Shepson, P. B.; Stirm, B. H.; Pratt, K. A. Springtime Bromine Activation over Coastal and Inland Arctic Snowpacks. *ACS Earth Space Chem.* **2018**, 2 (10), 1075–1086.
- (13) Foster, K. L.; Plastridge, R. A.; Bottenheim, J. W.; Shepson, P. B.; Finlayson-Pitts, B. J.; Spicer, C. W. The Role of Br2 and Brcl in Surface Ozone Destruction at Polar Sunrise. *Science* (1979) **2001**, 291 (5503), 471–474.
- (14) Custard, K. D.; Raso, A. R. W.; Shepson, P. B.; Staebler, R. M.; Pratt, K. A. Production and Release of Molecular Bromine and Chlorine from the Arctic Coastal Snowpack. ACS Earth Space Chem. 2017, 1, 142–151.
- (15) Pratt, K. A.; Custard, K. D.; Shepson, P. B.; Douglas, T. A.; Pöhler, D.; General, S.; Zielcke, J.; Simpson, W. R.; Platt, U.; Tanner, D. J.; Gregory Huey, L.; Carlsen, M.; Stirm, B. H. Photochemical Production of Molecular Bromine in Arctic Surface Snowpacks. *Nat. Geosci* 2013, 6 (5), 351–356.
- (16) Halfacre, J. W.; Shepson, P. B.; Pratt, K. A. PH-Dependent Production of Molecular Chlorine, Bromine, and Iodine from Frozen Saline Surfaces. *Atmos Chem. Phys.* **2019**, *19* (7), 4917–4931.
- (17) Wren, S. N.; Donaldson, D. J.; Abbatt, J. P. D. Photochemical Chlorine and Bromine Activation from Artificial Saline Snow. *Atmos Chem. Phys.* **2013**, *13* (19), 9789–9800.
- (18) Domine, F.; Sparapani, R.; Ianniello, A.; Beine, H. J. The Origin of Sea Salt in Snow on Arctic Sea Ice and in Coastal Regions. *Atmos. Chem. Phys.* **2004**, *4*, 2259–2271.
- (19) Peterson, P. K.; Hartwig, M.; May, N. W.; Schwartz, E.; Rigor, I.; Ermold, W.; Steele, M.; Morison, J. H.; Nghiem, S. V.; Pratt, K. A. Snowpack Measurements Suggest Role for Multi-Year Sea Ice Regions in Arctic Atmospheric Bromine and Chlorine Chemistry. *Elementa* **2019**, *7* (14), 1.
- (20) Simpson, W. R.; Alvarez-Aviles, L.; Douglas, T. A.; Sturm, M.; Dominé, F. Halogens in the Coastal Snow Pack near Barrow, Alaska: Evidence for Active Bromine Air-Snow Chemistry during Springtime. *Geophys. Res. Lett.* **2005**, 32 (4), 1–4.
- (21) Hara, K.; Osada, K.; Matsunaga, K.; Iwasaka, Y.; Shibata, T.; Furuya, K. Atmospheric Inorganic Chlorine and Bromine Species in Arctic Boundary Layer of the Winter/Spring. *Journal of Geophysical Research Atmospheres* **2002**, *107* (18), 1–15.
- (22) Bartels-Rausch, T.; Jacobi, H. W.; Kahan, T. F.; Thomas, J. L.; Thomson, E. S.; Abbatt, J. P. D.; Ammann, M.; Blackford, J. R.; Bluhm, H.; Boxe, C.; Domine, F.; Frey, M. M.; Gladich, I.; Guzmán, M. I.; Heger, D.; Huthwelker, T.; Klán, P.; Kuhs, W. F.; Kuo, M. H.; Maus, S.; Moussa, S. G.; McNeill, V. F.; Newberg, J. T.; Pettersson, J. B. C.; Roeselová, M.; Sodeau, J. R. A Review of Air-Ice Chemical and Physical Interactions (AICI): Liquids, Quasi-Liquids, and Solids in Snow. *Atmos Chem. Phys.* **2014**, *14* (3), 1587–1633.
- (23) Halfacre, J. W.; Shepson, P. B.; Pratt, K. A. PH-Dependent Production of Molecular Chlorine, Bromine, and Iodine from Frozen Saline Surfaces. *Atmos Chem. Phys.* **2019**, *19* (7), 4917–4931.
- (24) Custard, K. D.; Raso, A. R. W.; Shepson, P. B.; Staebler, R. M.; Pratt, K. A. Production and Release of Molecular Bromine and Chlorine from the Arctic Coastal Snowpack. *ACS Earth Space Chem.* **2017**, *1*, 142–151.
- (25) Fan, S.; Jacob, D. J. Surface Ozone Depletion in Arctic Spring Sustained by Bromine Reactions on Aerosols. *Nature* **1992**, *359*, 522–524.
- (26) Wang, S.; McNamara, S. M.; Moore, C. W.; Obrist, D.; Steffen, A.; Shepson, P. B.; Staebler, R. M.; Raso, A. R. W.; Pratt, K. A. Direct Detection of Atmospheric Atomic Bromine Leading to Mercury and

- Ozone Depletion. Proc. Natl. Acad. Sci. U. S. A. 2019, 116 (29), 14479–14484.
- (27) Simpson, W. R.; von Glasow, R.; Riedel, K.; Anderson, P.; Ariya, P. A.; Bottenheim, J. W.; Burrows, J. P.; Carpenter, L. J.; et al. Halogens and Their Role in Polar Boundary-Layer Ozone Depletion. *Atmos Chem. Phys.* **2007**, *7*, 4375–4418.
- (28) Simpson, W. R.; Brown, S. S.; Saiz-Lopez, A.; Thornton, J. A.; Von Glasow, R. Tropospheric Halogen Chemistry: Sources, Cycling, and Impacts. *Chem. Rev.* **2015**, *115* (10), 4035–4062.
- (29) Ariya, P. A.; Amyot, M.; Dastoor, A.; Deeds, D.; Feinberg, A.; Kos, G.; Poulain, A.; Ryjkov, A.; Semeniuk, K.; Subir, M.; Toyota, K. Mercury Physicochemical and Biogeochemical Transformation in the Atmosphere and at Atmospheric Interfaces: A Review and Future Directions. *Chem. Rev.* **2015**, *115* (10), 3760–3802.
- (30) Steffen, A.; Bottenheim, J.; Cole, A.; Douglas, T. A.; Ebinghaus, R.; Friess, U.; Netcheva, S.; Nghiem, S.; Sihler, H.; Staebler, R. Atmospheric Mercury over Sea Ice during the OASIS-2009 Campaign. *Atmos Chem. Phys.* **2013**, *13* (14), 7007–7021.
- (31) Schroeder, W. H.; Anlauf, K. G.; Barrie, L. A.; Lu, J. Y.; Steffen, A.; Schneeberger, D. R.; Berg, T. Arctic Springtime Depletion of Mercury. *Nature* **1998**, 394 (6691), 331–332.
- (32) McConnell, J. C.; Henderson, G. S.; Barrie, L. A.; Bottenheim, J. W.; Niki, H.; Langford, C. H.; Templeton, E. M. J. Photochemical Bromine Production Implicated in Arctic Boundary-Layer Ozone Depletion. *Nature* **1992**, 355, 150–152.
- (33) Barrie, L. A.; Bottenheim, J. W.; Schnell, R. C.; Crutzen, P. J.; Rasmussen, R. A. Ozone Destruction and Photochemical Reactions at Polar Sunrise in the Lower Arctic Atmosphere. *Nature* **1988**, 334 (6178), 138–141.
- (34) Wang, S.; Pratt, K. A. Molecular Halogens Above the Arctic Snowpack: Emissions, Diurnal Variations, and Recycling Mechanisms. *Journal of Geophysical Research: Atmospheres* **2017**, *122* (21), 11,991–12,007.
- (35) McNamara, S. M.; Garner, N. M.; Wang, S.; Raso, A. R. W.; Thanekar, S.; Barget, A. J.; Fuentes, J. D.; Shepson, P. B.; Pratt, K. A. Bromine Chloride in the Coastal Arctic: Diel Patterns and Production Mechanisms. *ACS Earth Space Chem.* **2020**, *4*, 620–630.
- (36) Le Bras, G.; Platt, U. A Possible Mechanism for Combined Chlorine and Bromine Catalyzed Destruction of Tropospheric Ozone in the Arctic. *Geophys. Res. Lett.* **1995**, 22 (5), 599–602.
- (37) Simpson, W. R.; von Glasow, R.; Riedel, K.; Anderson, P.; Ariya, P. A.; Bottenheim, J. W.; Burrows, J. P.; Carpenter, L. J.; et al. Halogens and Their Role in Polar Boundary-Layer Ozone Depletion. *Atmos Chem. Phys.* **2007**, *7*, 4375–4418.
- (38) Berg, W. W.; Sperry, P. D.; Rahn, K. A.; Gladney, E. S. Atmospheric Bromine in the Arctic. *J. Geophys Res.* **1983**, 88 (C11), 6719–6736.
- (39) Richter, A.; Wittrock, F.; Eisinger, M.; Burrows, J. P. GOME Observations of Tropospheric BrO in Northern Hemispheric Spring and Summer 1997. *Geophys. Res. Lett.* **1998**, 25 (14), 2683–2686.
- (40) Burd, J. A.; Peterson, P. K.; Nghiem, S. V.; Perovich, D. K.; Simpson, W. R. Snowmelt Onset Hinders Bromine Monoxide Heterogeneous Recycling in the Arctic. *J. Geophys Res.* **2017**, *122* (15), 8297–8309.
- (41) May, N. W.; Quinn, P. K.; Mcnamara, S. M.; Pratt, K. A. Multiyear Study of the Dependence of Sea Salt Aerosol on Wind Speed and Sea Ice Conditions in the Coastal Arctic. *Journal of Geophysical Research: Atmospheres* **2016**, *121*, 9208–9219.
- (42) McNamara, S. M.; Garner, N. M.; Wang, S.; Raso, A. R. W.; Thanekar, S.; Barget, A. J.; Fuentes, J. D.; Shepson, P. B.; Pratt, K. A. Bromine Chloride in the Coastal Arctic: Diel Patterns and Production Mechanisms. *ACS Earth Space Chem.* **2020**, *4* (4), 620–630.
- (43) McNamara, S. M.; Raso, A. R. W.; Wang, S.; Thanekar, S.; Boone, E. J.; Kolesar, K. R.; Peterson, P. K.; Simpson, W. R.; Fuentes, J. D.; Shepson, P. B.; Pratt, K. A. Springtime Nitrogen Oxide-Influenced Chlorine Chemistry in the Coastal Arctic. *Environ. Sci. Technol.* 2019, 53 (14), 8057–8067.
- (44) Liao, J.; Sihler, H.; Huey, L. G.; Neuman, J. A.; Tanner, D. J.; Friess, U.; Platt, U.; Flocke, F. M.; Orlando, J. J.; Shepson, P. B.;

- Beine, H. J.; Weinheimer, A. J.; Sjostedt, S. J.; Nowak, J. B.; Knapp, D. J.; Staebler, R. M.; Zheng, W.; Sander, R.; Hall, S. R.; Ullmann, K. A Comparison of Arctic BrO Measurements by Chemical Ionization Mass Spectrometry and Long Path-Differential Optical Absorption Spectroscopy. *Journal of Geophysical Research Atmospheres* **2011**, *116* (1), 1–14.
- (45) Tanner, D. J.; Jefferson, A.; Eisele, F. L. Selected Ion Chemical Ionization Mass Spectrometric Measurement of OH. *Journal Of Geophysical Research-Atmospheres* **1997**, *102* (D5), 6415–6425.
- (46) Huey, L. G.; Tanner, D. J.; Slusher, D. L.; Dibb, J. E.; Arimoto, R.; Chen, G.; Davis, D.; Buhr, M. P.; Nowak, J. B.; Mauldin, R. L.; Eisele, F. L.; Kosciuch, E. CIMS Measurements of HNO3 and SO2 at the South Pole during ISCAT 2000. *Atmos. Environ.* **2004**, *38* (32), 5411–5421.
- (47) Neuman, J. A.; Nowak, J. B.; Huey, L. G.; Burkholder, J. B.; Dibb, J. E.; Holloway, J. S.; Liao, J.; Peischl, J.; Roberts, J. M.; Ryerson, T. B.; Scheuer, E.; Stark, H.; Stickel, R. E.; Tanner, D. J.; Weinheimer, A. J. Bromine Measurements in Ozone Depleted Air over the Arctic Ocean. *Atmos Chem. Phys.* **2010**, *10* (14), 6503–6514.
- (48) Liao, J.; Huey, L. G.; Tanner, D. J.; Brough, N.; Brooks, S.; Dibb, J. E.; Stutz, J.; Thomas, J. L.; Lefer, B.; Haman, C.; Gorham, K. Observations of Hydroxyl and Peroxy Radicals and the Impact of BrO at Summit, Greenland in 2007 and 2008. *Atmos Chem. Phys.* **2011**, *11* (16), 8577–8591.
- (49) Peterson, P. K.; Simpson, W. R.; Pratt, K. A.; Shepson, P. B.; Frieß, U.; Zielcke, J.; Platt, U.; Walsh, S. J.; Nghiem, S. V. Dependence of the Vertical Distribution of Bromine Monoxide in the Lower Troposphere on Meteorological Factors Such as Wind Speed and Stability. *Atmos Chem. Phys.* **2015**, *15* (4), 2119–2137.
- (50) Liao, J.; Huey, L. G.; Tanner, D. J.; Flocke, F. M.; Orlando, J. J.; Neuman, J. A.; Nowak, J. B.; Weinheimer, A. J.; Hall, S. R.; Smith, J. N.; Fried, A.; Staebler, R. M.; Wang, Y.; Koo, J. H.; Cantrell, C. A.; Weibring, P.; Walega, J.; Knapp, D. J.; Shepson, P. B.; Stephens, C. R. Observations of Inorganic Bromine (HOBr, BrO, and Br2) Speciation at Barrow, Alaska, in Spring 2009. *Journal of Geophysical Research Atmospheres* 2012, 117 (D14), D00R16.
- (51) Quinn, P. K.; Miller, T. L.; Bates, T. S.; Ogren, J. A.; Andrews, E.; Shaw, G. E. A 3-Year Record of Simultaneously Measured Aerosol Chemical and Optical Properties at Barrow, Alaska. *Journal of Geophysical Research: Atmospheres* **2002**, *107* (D11), AAC 8-1.
- (52) Krnavek, L.; Simpson, W. R.; Carlson, D.; Dominé, F.; Douglas, T. A.; Sturm, M. The Chemical Composition of Surface Snow in the Arctic: Examining Marine, Terrestrial, and Atmospheric Influences. *Atmos. Environ.* **2012**, *50* (4), 349–359.
- (53) Newberg, J. T.; Matthew, B. M.; Anastasio, C. Chloride and Bromide Depletions in Sea-Salt Particles over the Northeastern Pacific Ocean. *J. Geophys Res.* **2005**, *110* (D6), 1–13.
- (54) Sturm, M.; Stuefer, S. Wind-Blown Flux Rates Derived from Drifts at Arctic Snow Fences. *Journal of Glaciology* **2013**, 59 (213), 21–34.
- (55) Toyota, K.; McConnell, J. C.; Staebler, R. M.; Dastoor, A. P. Air-Snowpack Exchange of Bromine, Ozone and Mercury in the Springtime Arctic Simulated by the 1-D Model PHANTAS Part 1: In-Snow Bromine Activation and Its Impact on Ozone. *Atmos Chem. Phys.* **2014**, *14* (8), 4101–4133.
- (56) France, J. L.; Reay, H. J.; King, M. D.; Voisin, D.; Jacobi, H. W.; Domine, F.; Beine, H.; Anastasio, C.; MacArthur, A.; Lee-Taylor, J. Hydroxyl Radical and NOx Production Rates, Black Carbon Concentrations and Light-Absorbing Impurities in Snow from Field Measurements of Light Penetration and Nadir Reflectivity of Onshore and Offshore Coastal Alaskan Snow. *Journal of Geophysical Research Atmospheres* 2012, 117 (D14), 1.
- (57) Krnavek, L.; Simpson, W. R.; Carlson, D.; Dominé, F.; Douglas, T. A.; Sturm, M. The Chemical Composition of Surface Snow in the Arctic: Examining Marine, Terrestrial, and Atmospheric Influences. *Atmos. Environ.* **2012**, *50* (4), 349–359.
- (58) Toom-Sauntry, D.; Barrie, L. A. Chemical Composition of Snowfall in the High Arctic: 1990 1994. *Atmos. Environ.* **2002**, *36*, 2683–2693.

- (59) Simpson, W. R.; Alvarez-Aviles, L.; Douglas, T. A.; Sturm, M.; Dominé, F. Halogens in the Coastal Snow Pack near Barrow, Alaska: Evidence for Active Bromine Air-Snow Chemistry during Springtime. *Geophys. Res. Lett.* **2005**, 32 (4), 1–4.
- (60) Toom-Sauntry, D.; Barrie, L. A. Chemical Composition of Snowfall in the High Arctic: 1990 1994. *Atmos. Environ.* **2002**, *36*, 2683–2693.
- (61) Cho, H.; Shepson, P. B.; Barrie, L. A.; Cowin, J. P.; Zaveri, R. NMR Investigation of the Quasi-Brine Layer in Ice/Brine Mixtures. *J. Phys. Chem. B* **2002**, *106* (43), 11226–11232.
- (62) MacDougall, D.; Crummett, W. B.; et al. Guidelines for Data Acquisition and Data Quality Evaluation in Environmental Chemistry. *Anal. Chem.* **1980**, 52 (14), 2242–2249.
- (63) Huff, A. K.; Abbatt, J. P. D. Kinetics and Product Yields in the Heterogeneous Reactions of HOBr with Ice Surfaces Containing NaBr and NaCl. J. Phys. Chem. A 2002, 106 (21), 5279–5287.
- (64) Adams, J. W.; Holmes, N. S.; Crowley, J. N. Uptake and Reaction of HOBr on Frozen and Dry NaCl/NaBr Surfaces between 253 and 233 K. *Atmos Chem. Phys.* **2002**, 2 (1), 79–91.
- (65) Sjostedt, S. J.; Abbatt, J. P. D. Release of Gas-Phase Halogens from Sodium Halide Substrates: Heterogeneous Oxidation of Frozen Solutions and Desiccated Salts by Hydroxyl Radicals. *Environ. Res. Lett.* **2008**, 3 (4), 045007.
- (66) Dominé, F.; Taillandier, A. S.; Simpson, W. R. A Parameterization of the Specific Surface Area of Seasonal Snow for Field Use and for Models of Snowpack Evolution. *J. Geophys Res. Earth Surf.* **2007**, *112* (2), 1–13.
- (67) Edebeli, J.; Trachsel, J. C.; Avak, S. E.; Ammann, M.; Schneebeli, M.; Eichler, A.; Bartels-Rausch, T. Snow Heterogeneous Reactivity of Bromide with Ozone Lost during Snow Metamorphism. *Atmos Chem. Phys.* **2020**, *20* (21), 13443–13454.
- (68) Kahan, T. F.; Kwamena, N. O. A.; Donaldson, D. J. Different Photolysis Kinetics at the Surface of Frozen Freshwater vs. Frozen Salt Solutions. *Atmos Chem. Phys.* **2010**, *10* (22), 10917–10922.
- (69) Takenaka, N.; Ueda, A.; Daimon, T.; Bandow, H.; Dohmaru, T.; Maeda, Y. Acceleration Mechanism of Chemical Reaction by Freezing: The Reaction of Nitrous Acid with Dissolved Oxygen. *J. Phys. Chem.* **1996**, *100* (32), 13874–13884.
- (70) Bales, R. C.; Davis, R. E.; Stanley, D. A. Ion Elution through Shallow Homogeneous Snow. *Water Resour Res.* **1989**, 25 (8), 1869–1877.
- (71) Johannessen, M.; Henriksen, A. Chemistry of Snow Meltwater: Changes in Concentration During Melting. *Water Resour Res.* **1978**, 14 (4), 615–619.
- (72) Peterson, P. K.; Pöhler, D.; Sihler, H.; Zielcke, J.; General, S.; Frieß, U.; Platt, U.; Simpson, W. R.; Nghiem, S. V.; Shepson, P. B.; Stirm, B. H.; Dhaniyala, S.; Wagner, T.; Caulton, D. R.; Fuentes, J. D.; Pratt, K. A. Observations of Bromine Monoxide Transport in the Arctic Sustained on Aerosol Particles. *Atmos Chem. Phys.* **2017**, *17* (12), 7567–7579.
- (73) Nissenson, P.; Packwood, D. M.; Hunt, S. W.; Finlayson-Pitts, B. J.; Dabdub, D. Probing the Sensitivity of Gaseous Br2 Production from the Oxidation of Aqueous Bromide-Containing Aerosols and Atmospheric Implications. *Atmos. Environ.* **2009**, 43 (25), 3951–3962.
- (74) Vogt, R.; Crutzen, P.; Sander, R. A Mechanism for Halogen Release from Sea-Salt. *Nature* **1996**, 383 (6598), 327–330.
- (75) Sturges, W. T.; Barrie, L. A. Chlorine, Bromine and Iodine in Arctic Aerosols. *Atmospheric Environment* **1988**, 22 (6), 1179.
- (76) Hara, K.; Osada, K.; Matsunaga, K.; Iwasaka, Y.; Shibata, T.; Furuya, K. Atmospheric Inorganic Chlorine and Bromine Species in Arctic Boundary Layer of the Winter/Spring. *Journal of Geophysical Research Atmospheres* **2002**, *107* (18), 1–15.
- (77) Ahmed, S.; Thomas, J. L.; Tuite, K.; Stutz, J.; Flocke, F.; Orlando, J. J.; Hornbrook, R. S.; Apel, E. C.; Emmons, L. K.; Helmig, D.; Boylan, P.; Huey, L. G.; Hall, S. R.; Ullmann, K.; Cantrell, C. A.; Fried, A. The Role of Snow in Controlling Halogen Chemistry and Boundary Layer Oxidation During Arctic Spring: A 1D Modeling

- Case Study. Journal of Geophysical Research: Atmospheres 2022, 127 (5), 1–29.
- (78) Sander, R.; Vogt, R.; Harris, G. W.; Crutzen, P. J. Modelling the Chemistry of Ozone, Halogen Compounds, and Hydrocarbons in the Arctic Troposphere during Spring. *Tellus B* **1993**, *49*, 522–532.
- (79) Yang, X.; Frey, M. M.; Rhodes, R. H.; Norris, S. J.; Brooks, I. M.; Anderson, P. S.; Nishimura, K.; Jones, A. E.; Wolff, E. W. Sea Salt Aerosol Production via Sublimating Wind-Blown Saline Snow Particles over Sea Ice: Parameterizations and Relevant Microphysical Mechanisms. *Atmos Chem. Phys.* **2019**, *19* (13), 8407–8424.
- (80) Yang, X.; Pyle, J. A.; Cox, R. A. Sea Salt Aerosol Production and Bromine Release: Role of Snow on Sea Ice. *Geophys. Res. Lett.* **2008**, 35 (16), 1–5.
- (81) Huang, J.; Jaeglé, L. Wintertime Enhancements of Sea Salt Aerosol in Polar Regions Consistent with a Sea Ice Source from Blowing Snow. *Atmos Chem. Phys.* **2017**, *17* (5), 3699–3712.
- (82) Huang, J.; Jaeglé, L.; Shah, V. Using CALIOP to Constrain Blowing Snow Emissions of Sea Salt Aerosols over Arctic and Antarctic Sea Ice. *Atmos Chem. Phys.* **2018**, *18* (22), 16253–16269.
- (83) Newberg, J. T.; Matthew, B. M.; Anastasio, C. Chloride and Bromide Depletions in Sea-Salt Particles over the Northeastern Pacific Ocean. J. Geophys Res. 2005, 110 (6), 1–13.
- (84) Beine, H. J.; Allegrini, I.; Sparapani, R.; Ianniello, A.; Valentini, F. Three Years of Springtime Trace Gas and Particle Measurements at Ny-Ålesund, Svalbard. *Atmos. Environ.* **2001**, *35* (21), 3645–3658.
- (85) Ianniello, A.; Beine, H. J.; Sparapani, R.; Di Bari, F.; Allegrini, I.; Fuentes, J. D. Denuder Measurements of Gas and Aerosol Species above Arctic Snow Surfaces at Alert 2000. *Atmos. Environ.* **2002**, *36* (34), 5299–5309.
- (86) Li, S.-M.; Yokouchi, Y.; Barrie, L. A.; Muthuramu, K.; Shepson, P. B.; Bottenheim, J. W.; Sturges, W. T.; Landsberger, S. Organic and Inorganic Bromine Compounds and Their Composition in the Arctic Troposphere during Polar Sunrise. *J. Geophys Res.* **1994**, 99 (D12), 25415–25428.
- (87) Barrie, L. A.; Li, S. M.; Toom, D. L.; Landsberger, S.; Sturges, W. Lower Tropospheric Measurements of Halogens, Nitrates, and Sulphur Oxides during Polar Sunrise Experiment. *J. Geophys Res.* **1992**, 99 (D12), 25453–25467.
- (88) Guimbaud, C.; Grannas, A. M.; Shepson, P. B.; Fuentes, J. D.; Boudries, H.; Bottenheim, J. W.; Dominé, F.; Houdier, S.; Perrier, S.; Biesenthal, T. B.; Splawn, B. G. Snowpack Processing of Acetaldehyde and Acetone in the Arctic Atmospheric Boundary Layer. *Atmos. Environ.* **2002**, *36* (15–16), 2743–2752.
- (89) Raso, A. R. W.; Custard, K. D.; May, N. W.; Tanner, D.; Newburn, M. K.; Walker, L.; Moore, R. J.; Huey, L. G.; Alexander, L.; Shepson, P. B.; Pratt, K. A. Active Molecular Iodine Photochemistry in the Arctic. *Proc. Natl. Acad. Sci. U. S. A.* **2017**, *114* (38), 10053–10058.
- (90) Colbeck, S. C. Model of Wind Pumping for Layered Snow. *Journal of Glaciology* **1997**, 43 (143), 60–65.
- (91) Albert, M. R.; Grannas, A. M.; Bottenheim, J.; Shepson, P. B.; Perron, F. E. Processes and Properties of Snow-Air Transfer in the High Arctic with Application to Interstitial Ozone at Alert, Canada. *Atmos. Environ.* **2002**, *36* (15–16), 2779–2787.
- (92) Raso, A. R. W.; Custard, K. D.; May, N. W.; Tanner, D. J.; Newburn, M. K.; Walker, L.; Moore, R. J.; Huey, L. G.; Alexander, L.; Shepson, P. B.; Pratt, K. A. Active Molecular Iodine Photochemistry in the Arctic. *Proc. Natl. Acad. Sci. U. S. A.* **2017**, *114* (38), 10053–10058.
- (93) Jeffries, M. O.; Overland, J. E.; Perovich, D. K. The Arctic Shifts to a New Normal. *Phys. Today* **2013**, *66* (10), 35–40.
- (94) Stroeve, J. C.; Markus, T.; Boisvert, L. N.; Miller, J.; Barrett, A. Changes in Arctic Melt Season and Implications for Sea Ice Loss. *Geophys. Res. Lett.* **2014**, *41*, 1216–1225.
- (95) Overland, J. E.; Wang, M.; Walsh, J. E.; Stroeve, J. C. Future Arctic Climate Changes: Adaptation and Mitigation Time Scales. *Earths Future* **2014**, 2, 68–74.